https://doi.org/10.22226/2410-3535-2023-2-132-137

Nanocomposite thin-film structures based on a polyelectrolyte complex of chitosan and chitosan succinamide with SWCNT

R. B. Salikhov†, R. A. Zilberg, E. O. Bulysheva, A. D. Ostaltsova, T. R. Salikhov, Yu. B. Teres

†salikhovrb@yandex.ru.

Ufa University of Science and Technology, Ufa, 450076, Russia

The article is devoted to the study of nanocomposite thin films based on a polyelectrolyte complex of chitosan and chitosan succinamide (PEC). Single-walled carbon nanotubes (SWCNT) were used as fillers. Using the methods of cyclic voltammetry and electrochemical impedance spectroscopy, it was found that nanocomposite films have a larger effective surface area and electron transfer rate compared to polyelectrolyte complex films, which allows them to be further used in the electroanalysis of substances of various nature. The study of the surface of the nanocomposite structure of PEC with SWCNT using SEM showed that there are formations in the form of filaments formed by carbon nanotubes on it. Studying the nature of morphology is extremely important when creating sensory devices. Sensory sensitivity of resistive thin-film nanocomposite structures to air humidity and ammonia vapors was found. Based on these nanocomposite materials, samples of resistive thin-film structures were prepared, the dependences of the flowing current on the relative humidity of the air and the concentration of ammonia vapors were measured.

Keywords: polyelectrolyte complex of chitosan and chitosan succinate, single-walled carbon nanotubes, nanocomposite, humidity sensor, ammonia vapor sensor.

1. Introduction

In the modern world, synthetic materials have replaced natural materials in many areas of human activity, which have become widespread due to their lower cost and a wide variety of properties. Another important advantage of synthetic materials is the possibility of further improvement of existing ones, the creation of new materials and technologies for their production by selecting raw materials, their ratio in the raw mixture, called composition, and technological parameters [1]. Currently, there are still many problems associated with the manufacture of flexible humidity sensors with the necessary properties for large-scale production [2]. Obtaining new materials with sensory properties and creating sensors based on them for monitoring toxic and environmentally harmful gases is an urgent task of analytical instrumentation [3].

In the field of nanotechnology, one of the most popular areas of current research and development are polymer nanocomposites and the field of research covers a wide range of topics: nanoelectronics and polymer bionanomaterials. Polymer nanocomposites are an important category of materials demonstrating excellent physicochemical properties that are inaccessible to individual components acting alone [4–5]. In the study [6], the authors reported on the creation of a sensor platform based on the $WO_3/Ti_3C_2T_x$ nanocomposite for detecting NO_2 gas at room temperature. The article [7] is devoted to the study of nanocomposite thin films based on polyarylene phthalide. Single-walled carbon nanotubes and graphene oxide were used as fillers. Based on the studied films used as a transport layer, field-effect transistors were created.

To date, the most popular are electronic sensors, which must have high energy efficiency. Existing sensors, as a rule, are made on oxide materials and require heating during operation. In addition, they are very inertial, have long response and recovery times. This work is devoted to the search for new composite materials for these sensors with high speed, low power consumption, low hysteresis and cost-effectiveness [8–10].

Currently, a variety of humidity sensors from foreign and domestic manufacturers are presented on the market of control and measuring devices. These are both fast-acting detectors that provide high linearity of converting relative humidity into a unified electrical output signal, and inexpensive converters with a large error. The most well-known are polymer and film relative humidity sensors of the capacitor (capacitive) or resistive type [11]. Humidity measurement is extremely important both in conventional environmental monitoring and in the emerging digital health management [12]. The humidity sensor is an important class of chemical sensors and is widely used in environmental monitoring, food packaging, electronics, to create human comfort [13].

The most popular chemical sensors should also include sensors capable of detecting ammonia vapors in the air [14]. Ammonia (NH_3) vapors are toxic to farm animals and humans [15–16]. Even low concentrations of NH_3 can have serious consequences for human health, such as irritation of the eyes, respiratory tract and skin, causing dizziness, nausea and fatigue [17–18]. The need to develop ammonia vapor sensors in the air operating at room temperature remains relevant today.

Polyelectrolyte complexes have unique capabilities for assembling nanostructures with recognition properties,

which are increasingly being used in various electrochemical sensors [19 – 25]. PEC are spontaneously formed by mixing oppositely charged solutions of polyelectrolytes in water without the use of organic solvents, chemical crosslinking agents or surfactants [26]. If necessary, PEC can include relatively small molecules and even nanoparticles, such as platinum nanoparticles [27], graphene oxide and carbon nanotubes [28 – 29].

The purpose of this work was to study the electrophysical properties of new nanocomposite materials based on PEC with SWCNT and to study their sensory sensitivity to air humidity and ammonia vapor.

2. Experimental part

2.1. Equipment and devices

Cyclic voltammograms (CV) and electrochemical impedance spectra were recorded using an AutoLab PGSTAT 204 potentiostat/galvanostat equipped with a FRA 32M module (Metrohm AutoLab, Netherlands) with Nova software. Electrochemical measurements were carried out in a three-electrode cell consisting of a modified glass-carbon electrode with a diameter of 3 mm as a working electrode, a platinum plate as an antielectrode and Ag/AgCl (saturated KCl) as a reference electrode. All measurements were carried out at room temperature 22 ± 5°C.

In the experiments, the following power supplies were used for measurements: MASTESN, DS ROWER SUPPLY HYZ005D-2, universal voltmeter DMM4020 as an ammeter, sealed cap. The error of all electrical measurements did not exceed 1%.

Humidity was monitored using a DHT11 sensor (an error of up to 5%). Ammonia vapors were recorded through the MQ135 sensor (error up to 10%). Vacuum spraying of aluminum electrodes was carried out on the UVP-250 installation.

Studies of the microstructure of composite films and PEC films were carried out using a scanning electron microscope (SEM) TESCAN MIRA LMS. The thickness of thin polymer films was controlled based on AFM image analysis.

2.2. Materials and reagents

PEC of polysaccharide nature was prepared on the basis of polycation-chitosan hydrochloride and polyanion-sodium salt of chitosan succinamide (JSC "Bioprogress", Russia). The sodium salt of chitosan succinamide (molecular weight 200 kDa) was obtained from chitosan with a degree of deacetylation of 82% and a degree of modification by amino groups of 75%. Chitosan hydrochloride was taken in the form of a film obtained from a chitosan hydrochloric acid solution, which was prepared by dissolving 0.25 g of chitosan (molecular weight 30 kDa) with a deacetylation degree of 75% in 50 ml of 1% HCl solution. The films were dried in air, followed by vacuum drying to a constant mass. Aqueous dispersions of PEC were obtained at a temperature of 25°C by adding chitosan succinate (0.005%) to aqueous solutions of chitosan hydrochloride (0.005%) drop by drop with intensive stirring (500 rpm) with 2 min interval between the introduction of portions. When new portions of chitosan hydrochloride solution were added to the resulting solution, phase separation occurred (stable opalescence of the general system is formed). The region of existence of PEC particle dispersions of these polysaccharides is limited by a molar ratio equal to 0.1, above which, already in the process of mixing the components, precipitation of the complex is observed [30 – 31].

Nanocomposites were prepared by dissolving in 1 ml of PEC 0.001, 0.002 and 0.003 g SWCNT (diameter 0.7 –1.1 nm) (Sigma-Aldrich, USA), followed by holding for 60 minutes in an ultrasonic bath (Elmsonic One, operating frequency 35 kHz).

Solution 5.0 mM $[Fe(CN)_6]^{4-/3-}$ Redox vapors (1:1) were prepared using 0.1 M KCl aqueous solution as a background electrolyte. All aqueous solutions were prepared on deionized water (conductivity 0.1 mcm).

The relative humidity of the air and the concentration of ammonia vapors in the working chamber of the installation changed over time after placing a cup of warm water or ammonia solution in this chamber.

2.3. Modification GCE

To modify the GCE 0.3 μl of the PEC-SWCNT nanocomposite, the droplet method was applied to the prepared electrode surface, followed by drying at a temperature of 80°C under an infrared lamp for 6 minutes, then cooled at room temperature and voltammograms were recorded. Before each measurement, the surface of the SUE was polished for 1 min using a deaglomerated suspension based on Al_2O_3 (0.3 microns) and a polishing material Spec-Cloth Adhesive black disk 200 mm (Allied High Tech Products Inc., USA), followed by repeated washing of the electrode with deionized water and air drying at room temperature.

2.4. Experimental methodology

Voltammetric and electrochemical characteristics of the impedance of GCE, GCE/PEC, GCE/PEC-SWCNT electrodes were studied in a standard solution of 5 mM $[Fe(CN)_6]^{4-/3-}$ in 0.1 M solution of background electrolyte KCl. Solution $[Fe(CN)_6]^{4-/3-}$ a volume of 20 ml was placed in an electrochemical cell. The impedance spectra were recorded in the frequency range of alternating current from 50 kHz to 0.1 Hz, with an amplitude of 5 mV. CV was recorded in the potential range from 0.6 to 1.0 V with a scanning speed of 0.1 V/s. The data array for each sample consisted of five parallel measurements, which was enough to obtain reproducible results. The PEC-SWCNT nanocomposite was stored for 5 days in the refrigerator at a temperature of 4°C.

Multilayer structures of resistive sensors were obtained on the basis of PEC-SWCNT thin films (Fig. 1). In resistive sensors, a citall substrate was used as a substrate. Aluminum electrodes were applied to the sitall substrate from above by thermal spraying in a vacuum chamber on the UVP-250 installation with a thickness of about 400 – 500 nm, the gap was created using a shadow mask. For some samples, a PEC polymer film with SWCNT was applied to the area of the gap between the electrodes of 50 microns. The ohmic nature of the

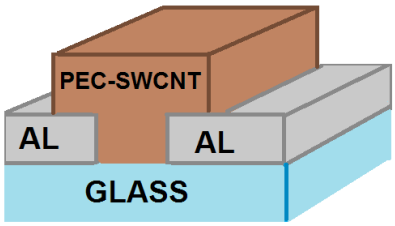

Fig. 1. (Color online) Structure of a thin-film resistive sensor.

contacts has been proven by measuring their current-voltage nature. The uniformity of the polymer surface in the working area of resistive sensors is confirmed by SEM studies. The resulting layer was subjected to thermal annealing to remove solvent residues by heating to 150°C for 20 – 25 minutes.

A sample of the humidity sensor was placed under a hood containing a control humidity sensor and a water container. The values of the input signal were taken at certain values of humidity or ammonia vapor concentration. Humidity was monitored using a DHT11 sensor (an error of up to 5%). Ammonia vapors were recorded through the MQ135 sensor (error up to 10%). A container with an aqueous solution of NH_3 was placed under a hood. Humidity values and ammonia vapor concentration values were taken via Arduino UNO and USB on the laptop screen. The measurements were carried out at room temperature 25°C, the voltage on the samples 30 V.

3. Results and discussion

When choosing the optimal composition of the composite based on PEC and SWCNT, the optimality criteria were the values of the maximum peak currents of the standard redox pair of the equimolar mixture of potassium hexacyanoferrate (II/III), charge transfer resistance (R_{et}), as well as their relative standard deviation during parallel measurements. Cyclic voltammograms describe a one-electron reversible redox process (Fig. 1a) of a redox pair $[Fe(CN)_6]^{3-/4-}$. Figure 1a shows that after the introduction of SWCNT into the PEC film, the peak currents of the redox pair $[Fe(CN)_6]^{3-/4-}$ on cyclic voltammograms increased compared to GCE/PEC. It is shown that with an increase in the SWCNT content in the range from 1 to 3 mg/ml, the oxidation peak current $[Fe(CN)_6]^{4-}$ increases (Fig. 1a). It can be assumed that this effect is associated with an increase in the effective surface area of the sensor (Table 1) and facilitating electron transfer to the electrode surface by adding SWCNT to the PEC. However, a further increase in the SWCNT content leads to an increase in the relative standard deviation and, consequently, to a decrease in the reproducibility of measurements, therefore, a composite containing 3 mg of SWCNT per 1 ml of PEC is chosen as optimal.

Effective sensor surface area (Table 1), calculated by the Randles-Shevchik equation [33] $I_p = (2.69 \times 10^5) n^{3/2} A D^{1/2} c \nu^{1/2}$, where I_p is the oxidation peak current, A; n is the number of transferred electrons ($n=1$); A is the electrode area, cm²; D is the diffusion coefficient ($D = 7.6 \times 10^{-6}$ cm²/s); c is the concentration of $K_4[Fe(CN)_6]$, mM; ν is the scanning speed ($\nu = 0.1$ V/s).

The electron transfer parameters were evaluated by electrochemical impedance spectroscopy. An equivalent Randles cell was used to quantify the impedance data. Figure 2b shows the corresponding Nyquist diagrams. The semicircle in the high frequency region corresponds to the limiting stage of charge transfer. The rectilinear section for modified electrodes in the region of lower frequencies describes the diffusion component of charge transfer [33]. Nyquist diagrams (Fig. 2b) indicate that GCE modified with a PEC film has a higher charge transfer resistance compared to composite sensors, which indicates that SWCNT dispersed in PEC are materials with good conductivity [34 – 36], and therefore the electron transfer rate has increased. It should be noted that with an increase in the SWCNT content in the composite from 1 to 3 mg/ml, a decrease in the charge transfer resistance is observed (Table 1), which is consistent with the data of the CV.

To study the stability, the nanocomposite was stored in a refrigerator at 4°C and a color of 5.0 mM solution was recorded

Table 1. Effective surface area and values of effective electron transfer resistance according to cyclic voltammetry and electrochemical impedance spectroscopy ($n=5$, $P=0.95$).

Sample	Clean PEC			PEC-SWCNT-3		
Scan are size, μm	4	8	100	4	8	100
Roughness, μm	0.07	0.08	0.08	0.1	0.1	0.11
Maximum peak height, μm	0.16	0.19	0.24	0.27	0.33	0.41

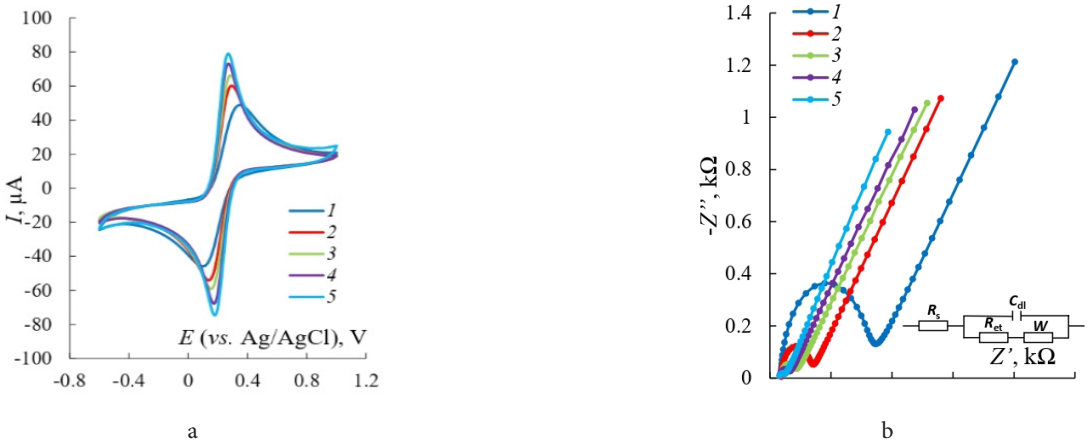

a b

Fig. 2. (Color online) Cyclic voltammograms (a) and Nyquist diagrams (b) for 5.0 mM solution $[Fe(CN)_6]^{3-/4-}$ on the background 0.1 M KCl on various electrodes:1 — GCE, 2 — GCE/PEC, 3 — GCE/PEC-SWCNT-1, 4 — GCE/PEC-SWCNT-2, 5 — GCE/PEC-SWCNT-3.

$[Fe(CN)_6]^{3-/4-}$ against a background of 0.1 M KCl every two days. The nanocomposite is stable for 5 days (Fig. 3), with longer storage, there is a decrease in peak currents and an increase in the relative standard deviation.

Images of the surface of the PEC and PEC-SWCNT-3 polymer under study were obtained using the TESCAN MIRA LMS scanning electron microscope (SEM) and the TESCAN Essence software (Fig. 4 a, b).

Unlike the surface of clean PEC, the surface of the PEC nanocomposite structure with SWCNT is covered with formations in the form of filaments. It can be assumed that these filaments are complex formations formed by carbon nanotubes.

The roughness values were obtained using the AFM image processing program Gwyddion [37]. The root mean square roughness and maximum peak height over the scanning area are given in Table 2. The surface roughness of nanocomposite structures is higher than the roughness of a pure polymer. Most likely, this is due to the presence of filamentous formations formed by carbon nanotubes, which is confirmed by SEM images.

The sensory sensitivity of the PEC-SWCNT-3 film to ammonia vapors in the air was also tested (Fig. 5.)

Films of PEC c SWCNT derivatives react to the presence of ammonia vapors in the environment by reducing the flowing current. The current decreases from a value of 260 μA to almost 140 μA when the concentration of ammonia vapor changes from 0 to 1000 mg/m³. The MPC of ammonia is 20 mg/m³. The characteristic is nonlinear: up to concentrations of 200 mg/m³, the current decreases quite quickly, then the rate of current reduction decreases sharply.

Let us try to explain our experimental results, which are associated with a decrease in the current passing through the resistive sample with an increase in the concentration of ammonia. There are two possible mechanisms: the first is associated with the charge transfer between ammonia molecules and the carbon nanotube, the second is

Table 2. Roughness values of samples.

Sensor	SWCNT content in the composite, mg/ml	A, mm²	R_{et}, Om
GCE	-	7.93 ± 0.06	768 ± 0.2
GCE / PEC	-	10.33 ± 0.06	250 ± 4.1
GCE / PEC-SWCNT-1	1	11.40 ± 0.07	131 ± 0.7
GCE / PEC-SWCNT-2	2	12.71 ± 0.08	81 ± 1.8
GCE / PEC-SWCNT-3	3	13.39 ± 0.08	47 ± 2.5

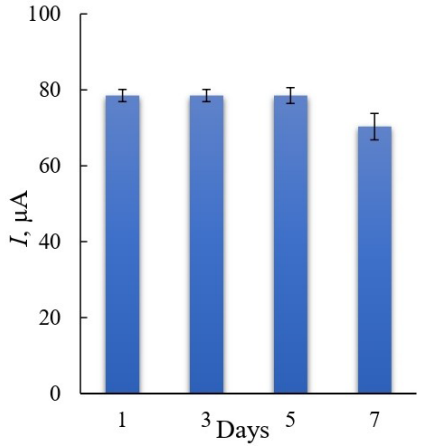

Fig. 3. GCE/PEC-SWCNT-3 sensor stability diagram. 5.0 mM solution was used $[Fe(CN)_6]3-/4-$ on the background 0.1 M KCl ($n = 5$, $P = 0.95$).

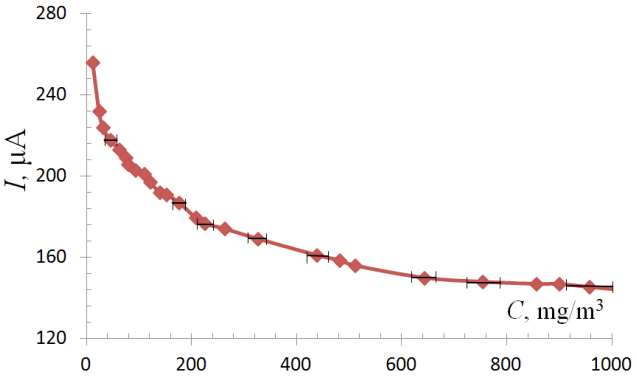

Fig. 5. Dependences of the current flowing through the PEC-SWCNT-3 films on the concentration of ammonia vapors in the air.

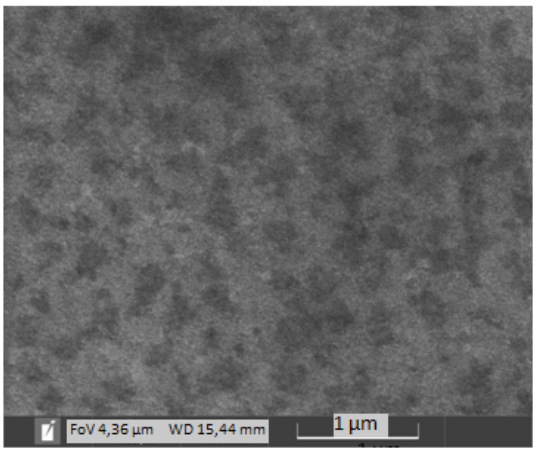

a

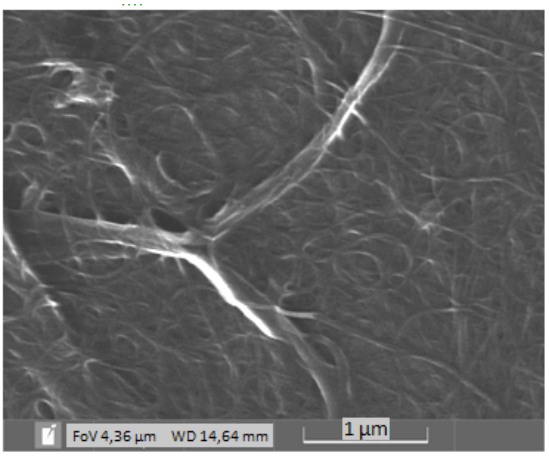

b

Fig. 4. SEM images of microstructures of film samples: pure PEC (a), PEC-SWCNT-3 (b).

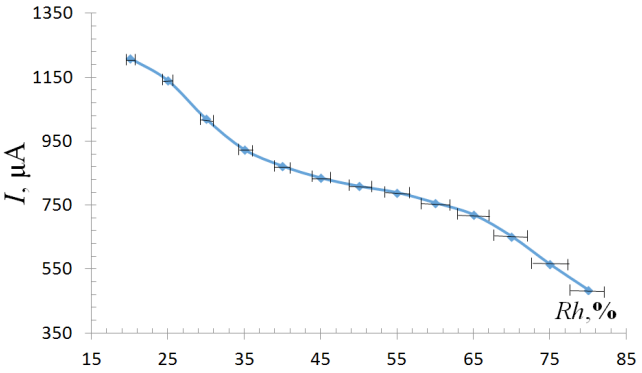

Fig. 6. Graphs of the dependence of the current flowing through the PEC-SWCNT-3 films on the relative humidity of the air.

associated with a change in the Schottky barrier between the nanocomposite film with nanotubes and the aluminum electrode [38]. In both mechanisms, the semiconductor nature of nanotubes is important. The interaction with oxygen molecules of the surrounding air is the cause of the hole conduction of nanotubes [39]. The adsorption of NH_3 by SWCNT defects can neutralize the positive charge due to the reduction effect and leads to an increase in the resistivity of nanotubes. Thus, the adsorption of NH_3 molecules continuously increases the electron density in the conduction band, compensating for the oxygen-induced hole density. In addition, there is another aspect of the decrease in current associated with an increase in resistance, due to an increase in the Schottky barrier. The adsorption of NH_3 molecules at the nanotube/Al interface reduces the output of the aluminum electrode, which leads to an increase in the Schottky barrier, which leads to a decrease in the level of injection of holes into the nanotube [40].

Based on the proposed PEC-SWCNT nanocomposite, an air humidity sensor has been developed. Figure 6 shows graphs of the dependence of the current flowing through the PEC films with SWCNT on the relative humidity of the air in the air volume.

The range of humidity changes was from 20% to 80% under the hood in the working chamber. The values of the current through the resistive sensor as the humidity increases are shown in Figure 6 and vary in the range from 450 to 1250 μA.

The dependence is not linear, the rate of decrease of the current value is approximately the same throughout the measurement range. The initial values of the current in Figs. 5,6 differ from each other in that the sensor samples differ in the thickness of the nanocomposite thin films used in them. The errors on the graph are not shown at all points, in order not to encumber Fig. 5. Current errors are not indicated, because they are not more than 1%.

As mentioned above, SWCNT usually exhibit hole conductivity and are p-type semiconductors [41]. Consequently, the reason for the increase in the electrical resistance of SWCNT due to the adsorption of water molecules may be that the adsorbed water molecules transfer electrons to the valence band of SWCNT, near the boundary of this zone, holes are transferred, as in any p-type semiconductors. The injection of electrons rapidly reduces the concentration of holes in the SWCNT, which leads to an increase in resistance. In addition, a decrease in the concentration of holes leads to an increase in the distance between the Fermi level and the valence band, which also causes a decrease in conductivity [42].

4. Conclusions

Using the methods of cyclic voltammetry and electrochemical impedance spectroscopy, it was found that nanocomposite films have a larger effective surface area and electron transfer rate compared to PEC films, which allows them to be further used in the electroanalysis of substances of various nature. It was found that the optimal content of SWCNT in PEC is 3 mg/ml. The PEC-SWCNT-3 nanocomposite is stable for 5 days.

Based on studies of the morphology of the surface of the PEC-SWCNT-3 nanocomposite structure using SEM, it is shown that it is covered with filamentous formations formed by carbon nanotubes. The sensory sensitivity of resistive thin-film nanocomposite structures to air humidity and ammonia vapors was detected and the dependences of the current flowing through these structures on the relative humidity of the air and the concentration of ammonia vapors were measured.

Acknowledgements. The research was funded with the support of a state assignment (scientific code FZWU-2023-0002) and the Russian Science Foundation (Grant No. 21-13-00169).

References

1. V. Vychuzhanin. Modern electronics. 5, 8 (2008). (in Russian)
2. M.K. Sokolskaya, A.S. Kolosova, I.A. Vitkalova, A.S. Orlova, E.S. Pikalov. Fundamental research. 10 (2), 290 (2017). (in Russian)
3. J. Wang, N. Wang, D. Xu, L. Tang, B. Sheng. Sensors and Actuators B: Chemical. 375, 132846 (2023). Crossref
4. I.D. Kosobudsky, K.V. Zapsis, N.M. Ushakov, V.Ya. Podvigalkin. Bulletin of the Saratov State Technical University. 1, 109 (2003). (in Russian)
5. Y. Xu, Z.Yan. Encyclopedia of Nanomaterials. 1, 306 (2023). Crossref
6. S. Gasso, A. Mahajan. Materials Science in Semiconductor Processing. 152, 107048 (2022). Crossref
7. R.B. Salikhov, R.A. Zilberg, I.N. Mullagaliev, T.R. Salikhov, Y.B. Teres. Mendeleev Communications, 32 (4), 520 (2022). Crossref
8. V.F. Markov, T.V. Vinogradova, I.V. Zarubin, L.N. Maskayeva. Analytics and control. 16 (4), 410 (2012). (in Russian)
9. R.B. Salikhov, V.Kh. Abdrakhmanov, T.T. Yumalin. International Ural Conference on Electrical Power Engineering. Proceedings — 2021 International Ural Conference on Electrical Power Engineering, UralCon 2021. (2021) p. 229. Crossref
10. A. Bunakov, A. Lachinov, R.B. Salikhov. Macromolecular Symposia. 212 (1), 387 (2004). Crossref
11. R.B. Salikhov, A.N. Lachinov, R.G. Rakhmeev, R.M. Gadiev, A.R. Yusupov, S.N. Salazkin. Measurement Techniques. 52 (4), 427 (2009). Crossref

12. Y. Yi, C. Yu, H. Zhai, L. Jin, D. Cheng, Y. Lu, Z. Chen, L. Xu, J. Li, Q. Song, P. Yue, Z. Liu, Y. Li. Nano Energy. 103 (A), 107780 (2022). Crossref
13. W. Xuan, X. He, J. Chen, W. Wang, X. Wang, Y. Xu, Z. Xu, Y. Q. Fu, J. K. Luo. Nanoscale. 7 (16), 7430 (2015). Crossref
14. X. Zhang, A. Wang, Y. Chen, J. Bao, H. Xing. Ecotoxicology and Environmental Safety. 248, 114325 (2022). Crossref
15. S. Manivannan, A. M. Saranya, B. Renganathan, D. Sastikumar, G. Gobi, K. C. Park. Sensors and Actuators B: Chemical. 171, 634 (2012). Crossref
16. D. Zhang, J. Wu, Y. Cao. Sens. Actuators B. 287, 346 – 355 (2019). Crossref
17. S. Bardócz. Trends Food Sci. Technol. 6 (10), 341 (1995). Crossref
18. B. Timmer, W. Olthuis, A. Van Den Berg. Sens. Actuators B Chem. 107, 666 (2005). Crossref
19. A. N. Ivanov, Yu. I. Kuzin, G. A. Evtugyn. Sensors and Actuators B: Chemical. 281, 574 (2019). Crossref
20. J. Lutkenhaus, P. Hammond. Soft. Matter. 3, 804 (2007). Crossref
21. G. Evtugyn, T. Hianik. TrAC Trends in Anal. Chem. 79, 168 (2016). Crossref
22. A. N. Malanina, Yu. I. Kuzin, A. N. Ivanov, G. K. Ziyatdinova, D. N. Shurpik, I. I. Stoikov, G. A. Evtyugin. Journal of Analytical Chemistry. 77 (2), 164 (2022). (in Russian) Crossref
23. Yu. A. Yarkaeva, D. I. Dubrovsky, R. A. Zilberg, V. N. Maistrenko. Journal of Analytical Chemistry. 75 (12), 1108 (2020). (in Russian) Crossref
24. R. A. Zilberg, T. V. Berestova, R. R. Gizatov. Inorganics. 10 (8), 117 (2022). Crossref
25. R. A. Zilberg, I. V. Vakulin, Yu. B. Teres, I. I. Galimov. Chirality. 34 (11), 1472 (2022). Crossref
26. D. Wu, L. Zhu, Y. Li, X. Zhang, S. Xu, G. Yang, T. Delair. Carbohydrate Polymers. 238 (15), 116126 (2020). Crossref
27. M. dos Santos, E. Wrobel, V. dos Santos, S. Quináia, S. Fujiwara, J. Garcia, C. A. Pessôa, E. W. Scheffer, K. Wohnrath. J. Electrochem. Soc. 163 (9), B499 (2016). Crossref
28. I. Škugor Rončević, D. Krivić, M. Buljac, N. Vladislavić, M. Buzuk. Polyelectrolytes Assembly: A Powerful Tool for Electrochemical Sensing Application. Sensors. 20 (11), 3211 (2020). Crossref
29. D. Prifitis. Curr. Org. Chem. 19, 1819 (2015). Crossref
30. S. V. Kolesov, M. S. Gurina, R. H. Mudarisova. High-molecular compounds. Series A. 61 (3), 195 (2019). (in Russian) Crossref
31. S. V. Kolesov, M. S. Gurina, R. H. Mudarisova. Journal of General Chemistry. 88 (8), 1376 (2018). (in Russian) Crossref
32. A. J. Bard, L. R. Faulkner. Electrochemical Methods. Fundamentals and Application, 2nd edn. New York (2004).
33. A. Lasia. Electrochemical Impedance Spectroscopy and its Applications. NewYork (2014). Crossref
34. G. K. Ziyatdinova, S. N. Shtykov, De Gruyter, H. C. Budnikov. Nanoanalytics: Nanoobjects and Nanotech-nologies in Analytical Chemistry. (2018) pp. 223 – 252.
35. M. A. Atieh, O. Y. Bakather, B. Al-tawbini, A. A. Bukhari, F. A. Abuilaiwi, M. B. Fettouhi. Bioinorg. Chem. Appl. 9, 603978 (2010). Crossref
36. P. M. Ajayan. Nanotubes from Carbon. Chem. Rev. 99, 1787 (1999). Crossref
37. A. R. Tuktarov, R. B. Salikhov, A. A. Khuzin, N. R. Popod'ko, I. N. Safargalin, I. N. Mullagaliev, U. M. Dzhemilev. RSC Advances, 9 (13), 7505 (2019). Crossref
38. J. Kong, N. R. Franklin, C. Zhou, M. G. Chapline, S. Peng, K. Cho, H. Dai. Science. 287, 622 (2000). Crossref
39. S. Z. Bisri, J. Gao, V. Derenskyi, W. Gomulya, I. Iezhokin, P. Gordiichuk, A. Herrmann, M. A. Loi. Adv. Mater. 24, 6147 (2012). Crossref
40. N. Peng, Q. Zhang, C. L. Chow, O. K. Tan, N. Marzari. Nano Lett. 9, 1626 (2009). Crossref
41. O. K. Varghese, P. D. Kichambre, D. Gong, K. G. Ong, E. C. Dickey, C. A. Grimes. Sens. Actuators B. 81, 32 (2001). Crossref
42. C. L. Cao, C. G. Hu, L. Fang, S. X. Wang, Y. S. Tian, C. Y. Pan. J. Nanomater. 2011 (10), 707303 (2011). Crossref